American Journal of Engineering Research (AJER)
e-ISSN: 2320-0847 p-ISSN: 2320-0936
Volume-12, Issue-8, pp-120-134
www.ajer.org
Research Paper Open Access

Natural-based composites Reinforced by Cellulose Nanofibers for removing heavy metals from the aquatic environment.

Hassan M. Alzain[1],
[1]*Environmental Protection Organization, Saudi Aramco, Al-Midra Tower, Dhahran 31311, Kingdom of Saudi Arabia*

Abstract
Using an electron beam (EB) at anirradiation dose of 20kGy, smart hydrogels were developedfrom Chitosan, acrylic-acid (AAc) and reinforced with varying ratios of cellulose nanofibers (CNF). These hydrogels of Chitosan-g-Poly(AAc)/CNF$_{0.1}$ were used to eliminate cadmium heavy metal from aqueous environment. A variety of analytical tools were used to evaluate the prepared hydrogels. Investigating swelling performance with time, medium pH, and CNF concentrations. The investigational results revealed that swelling percentage increases with a medium pH until it reaches equilibrium after 300 hours. The maximum swelling was achieved with Chitosan-g-Poly(AAc)/CNF$_{0.1}$ pH 10.The data also demonstrate that incorporating CNF into the hydrogel matrix enhanced its capacity in removing heavy metals (Cd^{++}). An ideal CNF concentration was 0.1Chitosan-g-Poly(AAc)/CNF$_{0.1}$.A structure with a higher CNF concentration is highly cross-linked and has a smaller amount of swellingbehaviors. Impact of temperature, and impact of time on the elimination percentage were examined. Theelimination percentage of chitosan-g-Poly(AAc)hydrogels decreases as time and increased with temperature fractions.
Keywords:*Chitosan, Cellulose Nano Fibers, Electron beam (EB), Polyacrylic acid, Heavy metal removal.*

Date of Submission: 01-08-2023 Date of acceptance: 12-08-2023

I. Introduction

Three-dimensional polymeric networks called hydrogels have a high-water content and are very flexible and insoluble in water **(Bryan et al., 2017).** Hydrogels are able to achieve the preferred adsorption character, high durability and stability during storage and swelling, high bio-degradability devoid ofdevelopment of hazardcompounds after bio-degradation, lack of color or odor, and low cost, among other characteristics. Hydrogels are widely used in a variety of industries, including agriculture, engineering, water treatment and biomedicine.Researchers' interest in creating hydrogels for environmental use has recently increased, especially in water remediation.The slightly cross-linked structure of hydrophilic hydrogels permits them to absorb water in their networks without dissolving **(Gonçalves et al., 2017)**. The adsorption properties of heavy metals and synthetic dyes is made more accessible by the existence of a few functional groups in hydrogels, such as carboxyl, hydroxyl, and amines **(Faheem et al., 2015)**.

Chitosan is existent normally in nature that is affordable, and biodegradable, which has prompted researchers to look into its potential use in different era**(Ahmad et al., 2014)**. The most famous water-absorbing substances is the acrylic acid (AAc). The swelling behavior of the poly-acrylic acid (PAAc) hydrogel is highly dependent on the pH of the surrounding medium due to the presence of COOH side groups **(Khawar et al., 2018)**. H-bonding between COOH group from pofly-acrylic acid and the OH groups of starch give Chitosan more stability when grafted onto it **(Mahamad et al., 2015)**. Utilizing nanomaterials like cellulose nanofibers (CNFs), it is possible to improve the poor mechanical characters and adsorption behaviors of hydrogels made from Chitosan. CNFs are extracted from various sources. The diameter range of the CNFs may be limited (5–100 nm). It was found that including CNFs improved the swelling capacity. In addition, 5 wt% CNFs assisted hydrogels had improved compressive strength and Young's modulus compared to un-reinforced ones **(Samiullah et al., 2018)**.

Without using a cross-linking agent or initiator, the polymer dissolves in an aqueous solution with the monomer dispersed in it. Then it goes through cross-linking and grafting to produce hydrogel via the electron beam technique for polymerization as a very effective tool **(Zahir et al., 2017)**. Numerous environmental issues have arisen due to the significant increase in discharged heavy metal pollutants brought on by the rapid development of industry **(Saravanan et al., 2013b)**. While some heavy metals are naturally occurring substances others can accumulate in the body and pose a risk to human health. Water effluents contain a variety of contaminants released due to various human activities. According to **(Gupta et al., 2014)**, metal mining, agricultural pesticide wastes, and industrial factory sewage are the main causes of heavy metal in aquatic environment.

Heavy metals pose numerousdangers to the all-inclusive eco-system, particularly to the whole food-chain cycle, such as cadmium, arsenic, lead, and mercury **(Saravanan et al., 2014a)**. The heavy metal cadmium (Cd) is linked to lung and kidney damage and is also thought to be a cancer-causing substance. Cd metal ions bring on mental retardation. Adsorption is the most frequently used method for removing heavy metal because of its high removal effectiveness and ease of use **(Saravanan et al., 2014b)**. The adsorbent in the adsorption process is essential for effective removal. Therefore, evolving new, high proficiency, cheap, and easy in preparationhydrogel has become the focal point in research **(Iram et al., 2019)**.

This study used the electron beam irradiation technique to create a variety of chitosan-g-PAAc and chitosan-g-PAAc/CNF hydrogels.Investigations were made into the characteristics and properties of the produced hydrogels.The hydrogels were utilized as adsorbents to remove the Cd (II) metal ion from the aqueous solution.We identified time and temperature as the main determinants of the prepared hydrogels' adsorption properties.

II. Materials and Methods

Chemicals

Sigma Aldrich, Germany, supplied Chitosan. Acrylic acid 99% (Merck, Germany) was used as received. Distilled water was used as a solvent, cellulose nanofibers-CNFs from National Research Center.Extra chemicals, such as $CdCl_2$, HNO_3, NaOH, and HCL were acquired from El-Nasr Co. (Cairo, Egypt).

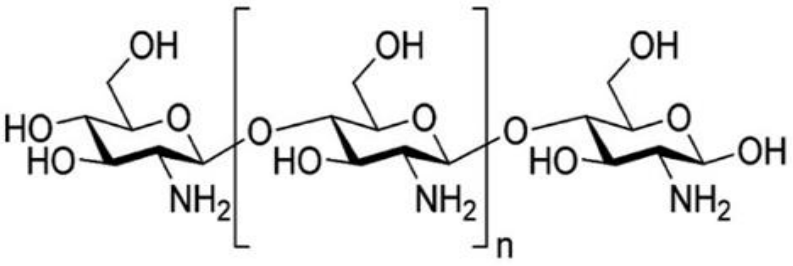

Chitosan

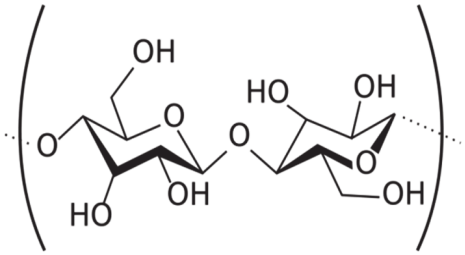

CNF

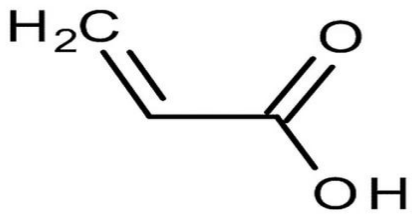

Acrylic acid

Characterization.

Instrumentations.

Irradiation technique.

Utilizing 3 MeV electron energy (energy instability: 2% maximum), 30 mA beam current (current instability: 2% maximum), and a 90 kW EB accelerator as the beam power, electron beam (EB) irradiation was performed

in ambient air. With an extraction window length of about 90 cm and a current of 10 mA, all samples were exposed to radiation; the controllable scan width ranged from 60 cm to the scanner's maximum width. The National Center for Radiation Research and Technology, Cairo, Egypt, exposed samples to doses of 10, 20, 30, 40, and 50 kGy radiation.

FTIR spectroscopic analysis

FTIR spectrophotometer was used Spectrum One, Perkin-Elmer/Waltham, MA, USA, over the range of 4000–400 cm^{-1} at a scan rate of 1spectrum/s at 4 cm^{-1} resolution.

Thermogravimetric analysis (TGA)

The TGA measurements were conducted on samples using (Perkin-Elmer Co., USA) at a heating rate of 10°C / 1 min from 100-600◦C under a nitrogen gas.

Transmission Electron Microscopy (TEM) Analysis

The particle size and morphology of CNF nanoparticles were calculated using a transmission electron microscope (JEOL, JEM100CS, Japan).

Scanning Electron Microscopy (SEM)

Using the SEM technique, the surface morphology of the samples was examined. The micrographs were captured using a Japanese scanning microscope (JEOL—JSM 5200 SCANNING MICROSCOPE) and voltage speeded up at 25 kV.

Preparation of PolyChitosan-g-PAAc/CNF hydrogel

Chitosan was completely dissolved in 2% acetic acid at 80 °C while being stirred in the presence of distilled water and a 1% concentration of chitosan. CS solutions with various monomer composition ratios (CS /AAc) of 1:2 wt%, 1:5 wt%, 1:10 wt%, and 1:15 wt% were added to 10 ml of dissolved Chitosan solution in various glass tubes. The glass tubes were tightly sealed before being exposed to gamma radiation at a dose rate of 0.56 Gy/sec and a dose of 20 kGy. The Egyptian Atomic Energy Authority (National Center for Radiation Research and Technology), located in Cairo, Egypt (the gamma irradiation facility).

Preparation of Chitosan-g-PAAc/CNF hydrogel

Different weights (0.05, 0.1, 0.15, and 0.2 gm.) of CNF were added to the mixture of Chitosan-AAc were gradually added in order to graft AAc monomers to the surface of Chitosan (where the total volume of each was 5ml). At room temperature, on a magnetic stirrer, the chitosan, AAc, and CNF mixture was stirred until the CNF was completely dissolved. A 20 kGy dose of radiation from an electron beam (EB) source was applied to the viscous solution after it had been poured into the glass tube. After the vials were broken following copolymerization, the formed polymeric cylinders were taken out and cut into discs with a 2 mm thickness and a 5 mm diameter. All samples were washed with distilled water to remove the unreacted constituents before being allowed to air dry at ambient temperature.

Gel percent

The (Gel %) was measured by using equation (1):

$$\text{Gel (\%)} = \frac{W_g}{W_0} X\ 100 \quad (1).$$

Where W_g and W_o were the weight of the dried sample after and before extractions, correspondingly.

Swelling studies

Swelling Behavior at Different Times

The hydrogel discs were soaked in distilled water at ambient atmosphere with a known weight. Gels that had swelled up were taken out of the water, dried, and weighed numerous times. The experiments were carried out for 240 hours or until a constant weight was achieved for each sample. The swelling percentage was calculated by using equation (2):

$$\text{Swelling (\%)} = \frac{W_s - W_d}{W_d} x100 \quad (2).$$

Where $W_s$and W_d are the weights of the swollen samples and the dried samples, correspondingly.

Adsorption study

In order to study the adsorption and removal ofCd (II)ions bythe hydrogels, different solutions of Cd (II)ions with various concentrations (C_0) (20, 40, 60, 80, and 100 mg/L) were employed; 0.05g of Each hydrogel was submerged in 20 ml of each of these solutions for 24 hours at 25 ^oC while stirring and maintaining at pH of 5. The hydrogel was then taken off, and an Agilent 5100 Inductively Coupled Plasma -Optical Emission Spectrophotometer (ICP-OES) with Synchronous Vertical Dual View (SVDV) was used to determine the final concentration of Cd (II) ions (C_f mg/L).The removal % was measuredby using equation (3);

$$\text{The removal (\%)} = \frac{C0-Cf}{C0} X100 \quad (3)$$

Impact of contact time on metal adsorption

0.05g of each hydrogel was put into a glass containing 20 mL of Cd (II) solution, which was adjusted to the optimum pH(pH=5) and then stirred with different time variations with variations in contact time of 15, 30, 60, 120, 180, 360,480, 720 and 1440 min. the mix were filtered then diluted with 0.1 M HNO_3 solution and then analyzed with (ICP-OES).

Impact of temperature on adsorption capacity

Each hydrogel with 0.5 g was mixed at a different temperature of 25, 40, and 60 oC after being added to glass ampoules containing 20 mL of a 20 mg/L Cd (II) solution that had been adjusted to the ideal (PH=5) concentration. Filtered mixture was then diluted with 0.1 M HNO3 solution and subjected to (ICPOES) analysis.

III. Results and discussion

Preparation of the hydrogel

Hydrogel can be prepared using the straightforward electron beam (EB) technique. Chitosan polymer and AAc monomer are dissolved in a solution that is exposed to an electron beam (EB), which causes water radiolysis and produces $(H)^{\cdot}$, $(OH)^{\cdot}$free radicals during the irradiation process. The macroradicals are created when the OH attacks the polymer chain. On AAc, free radicals begin to polymerize. Chitosan-g-Poly(AAc) hydrogel has a crosslinked chains structure attributable to the macroradicals' attack on the AAc. The CNF molecule can interact with Chitosan to create a Chitosan-g-Poly(AAc)/$CNF_{0.1}$ hydrogel product**(Randhawaet al., 2022)** as shown in Figure. 1. Based on earlier research, a fixed dose of the electron beam (EB) irradiation (20 KGy) was used to promote cross-linking and achieve the desired level.High irradiation doses are known to cause the development of highly cross-linked structures with undesirable properties**(Manas et al., 2018)**.

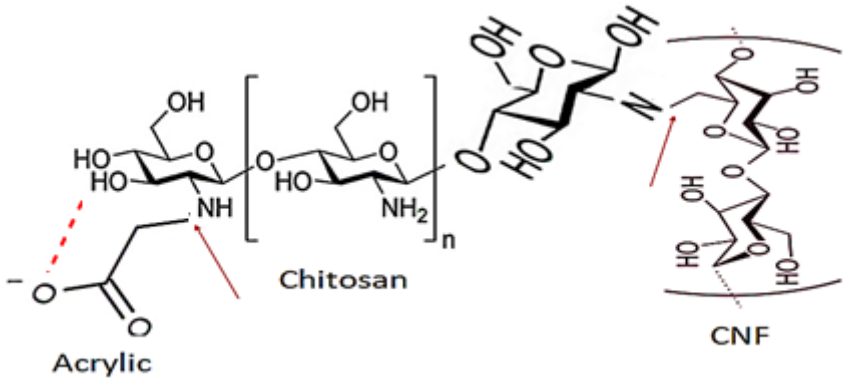

Figure (1):Schematic representation ofpotentialcross-linking between Chitosan, Polyacrylic acid, and CNF.

According to the observed outcomes, the gelation percent (Gel %) rises as the irradiation dose does rises. Figure 2a illustrates how the irradiation dose affected the gelation percentage. This behavior may be attributed to higher levels of crosslinking that develop in the hydrogel structure during the copolymerization process and an increase in the concentration of readily available free radicals.**(Sokker et al. 2009).**

It was discovered that the gelation percent (Gel %) extended its extreme value at an irradiation dose of 20 kGy.The gelation (%) slightly decreased as the irradiation-dose amended to 30 kg. This is because high radiation doses cause the cross-linking to degrade, and since Chitosan is a radiation-degradable polymer, the rate of degradation may be faster than the rate of crosslinking according to the irradiation doses exposure. From (Figure. 2b), the results are evident that gelation (%) increases as the ratio of (Chitosan: AAc)increases **(Bretel et al., 2018).**

The gelation percent (Gel %) reached its maximum value at 1:10 wt%. Chitosan: AAc ratio: This is because the rate of AAC monomer diffusion into the polymer matrix favors the growth of chains, which causes the gel % to increase. Above this ratio, the Gel% decreased, possibly because, at high AAC monomer concentrations, the rate of G (R) formation of the monomers is faster than the rate of monomer diffusion through the hydrogel matrix, which causes trapped radicals to recombine with one another.

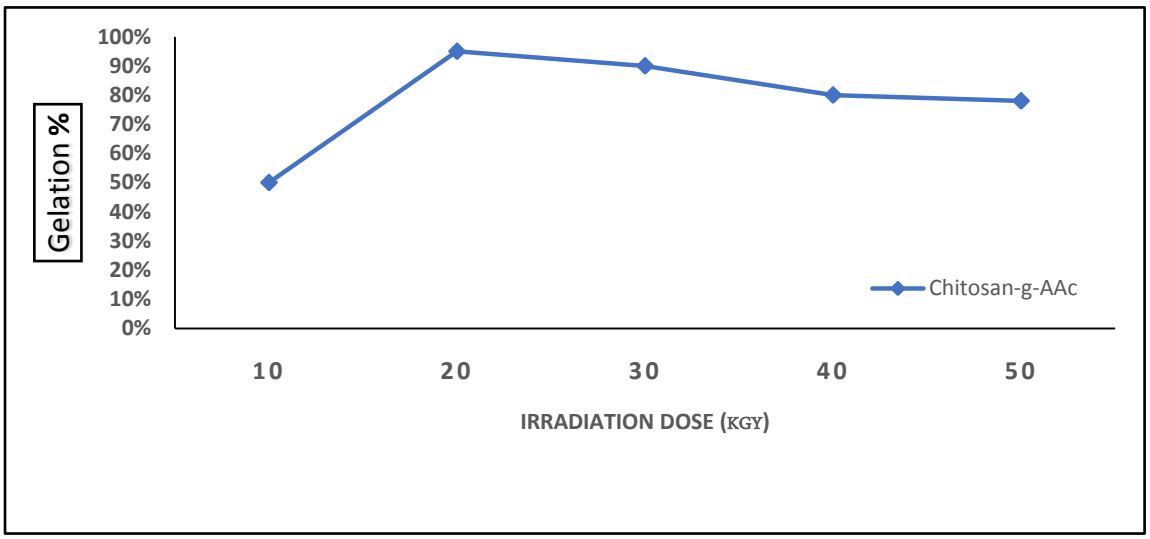

Figure (2):Effect of different irradiation doses on the gel (%) of Chitosan-g-Poly(AAc)hydrogel.

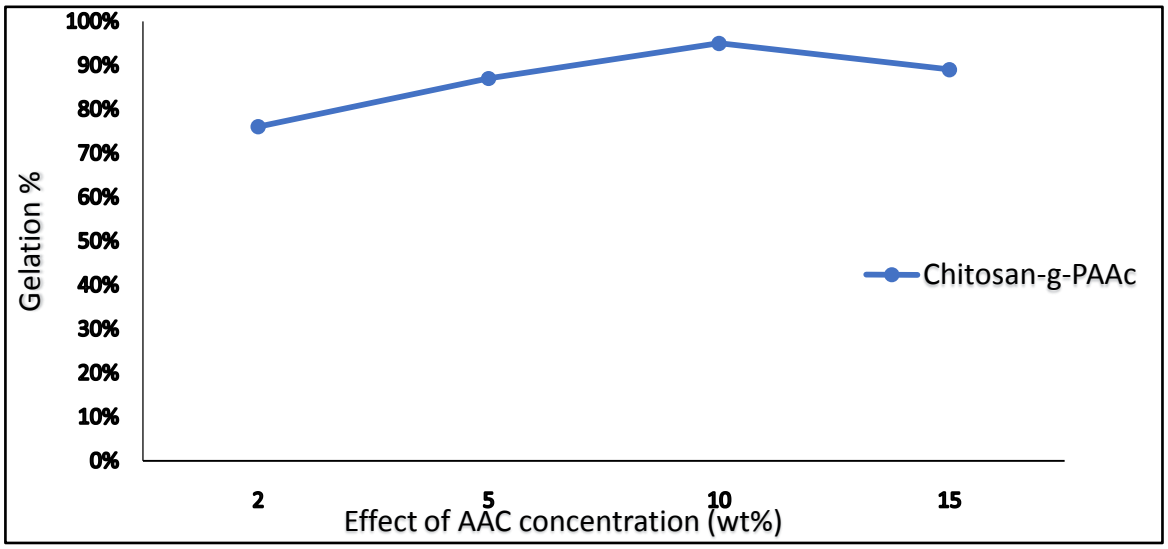

Figure(3):Impact of AAc contents on the gel (%) of Chitosan-g-Poly(AAc)hydrogel at Irradiation dose 20 kGy.

Effect of the concentration of (CNF) on gelation (%)

Figure 3 illustrates how the concentration of (CNF) affects the percentage of gelation. The observed outcomes demonstrate that the gelation percent (G %) increases as the concentration of (CNF) decreases, according to **(Huq et al., 2012)**. As a result of the strong H-bonding between nanofibers and the functions groups of the monomers initiated by the high concentration of hydroxyl groups in CNF, the available spaces are reduced, and the Gel% is raised.

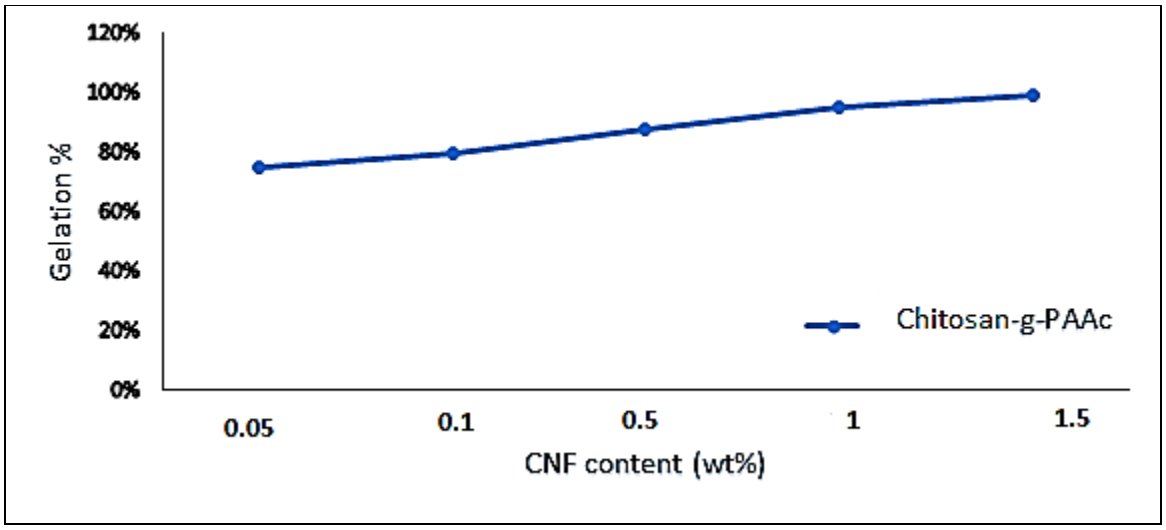

Figure (4):Impact of (CNF) content on the gel (%) of Chitosan-g-Poly(AAc) hydrogel.

Swelling Behavior

The swelling behavior of Chitosan-g-Poly(AAc)/$CNF_{0.1}$ hydrogels with various CNF contents is depicted in Figure 4a as a function of time. As can be noted in the Figure, Chitosan-g-Poly(AAc)/$CNF_{0.1}$ hydrogels exhibited high swelling property. This behavior was amplified over time, reaching equilibrium for all hydrogels after 250 hours. On the other hand, the Chitosan-g-Poly(AAc)/$CNF_{0.1}$ has a high swelling equilibrium **(Yang et al., 2014)**.

As shown in Figure 4(a, b), the existence of CNFs in the nanocomposite formula appeared to significantly impact the swelling capabilities of the Chitosan-g-Poly(AAc)/$CNF_{0.1}$ nanocomposite hydrogel. Due to the enhancement of function groups existence, which was accomplished by rising the concentration of CNFs, the hydrophilic character of Chitosan-g-Poly(AAc)/$CNF_{0.1}$ hydrogels was improved. However, as the CNF content rose in Chitosan-g-Poly(AAc)/$CNF_{0.15}$, a decline in the swelling% was seen. A higher CNF content could result in a more compact network structure and less room for water retention. Swelling character is crucial when using a material as an adsorbent. The swelling will increase proportionately to the number of function groups available on the network structure. Therefore, Chitosan-g-Poly(AAc)/$CNF_{0.1}$ composite was selected in the thisresearchdue to enhanced swelling characters **(Gharekhani et al., 2017)**.

Figure 4c shows the swelling characteristics of the Chitosan-g-Poly(AAc) and the Chitosan-g-Poly(AAc)/$CNF_{0.1}$, which contain 0.1 wt% CNFs. Both systems have a significant capacity for swelling. The swelling (%) of the Chitosan-g-Poly(AAc)/$CNF_{0.1}$ nanocomposite is greater than that of the Chitosan-g-Poly(AAc) hydrogel. Since CNF is full of hydrophilic groups like hydroxyl groups, the hydrophilicity character of the entire hydrogel matrix increases as time goes on due to its introduction**(Jayaramudu et al., 2017)**.

Figure 4d illustrates how pH affects how much the Chitosan-g-Poly(AAc)/$CNF_{0.1}$ hydrogel swells. Raising the pH from 2 to 10 for both hydrogels exacerbated the swelling. The COOH group is known to respond to the pH level. When placed in an acidic environment, the carboxylic group protonates up to pH 4.6, corresponding to PAAc'spKa value. Therefore, a further rise in pH causes de-protonation of the COOH. Due to the negatively charged carboxylate ions' attraction, more water molecules can be taken in, which improves the swelling's equilibrium **(Chang et al., 2021)**.

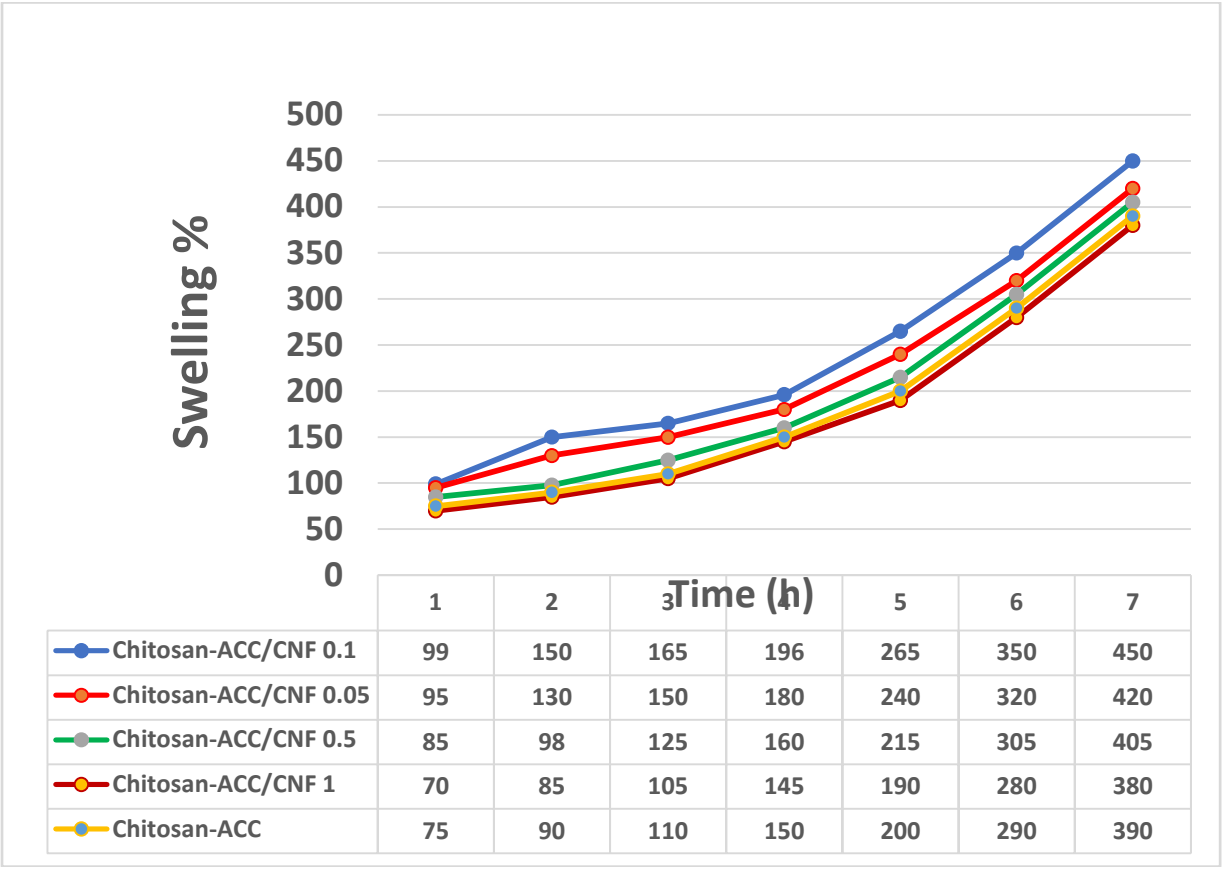

	1	2	3	4	5	6	7
Chitosan-ACC/CNF 0.1	99	150	165	196	265	350	450
Chitosan-ACC/CNF 0.05	95	130	150	180	240	320	420
Chitosan-ACC/CNF 0.5	85	98	125	160	215	305	405
Chitosan-ACC/CNF 1	70	85	105	145	190	280	380
Chitosan-ACC	75	90	110	150	200	290	390

Figure (5):Swelling behavior of Chitosan-g-Poly(AAc) and Chitosan-g-Poly(AAc)/CNF$_{0.1}$ hydrogels against time.

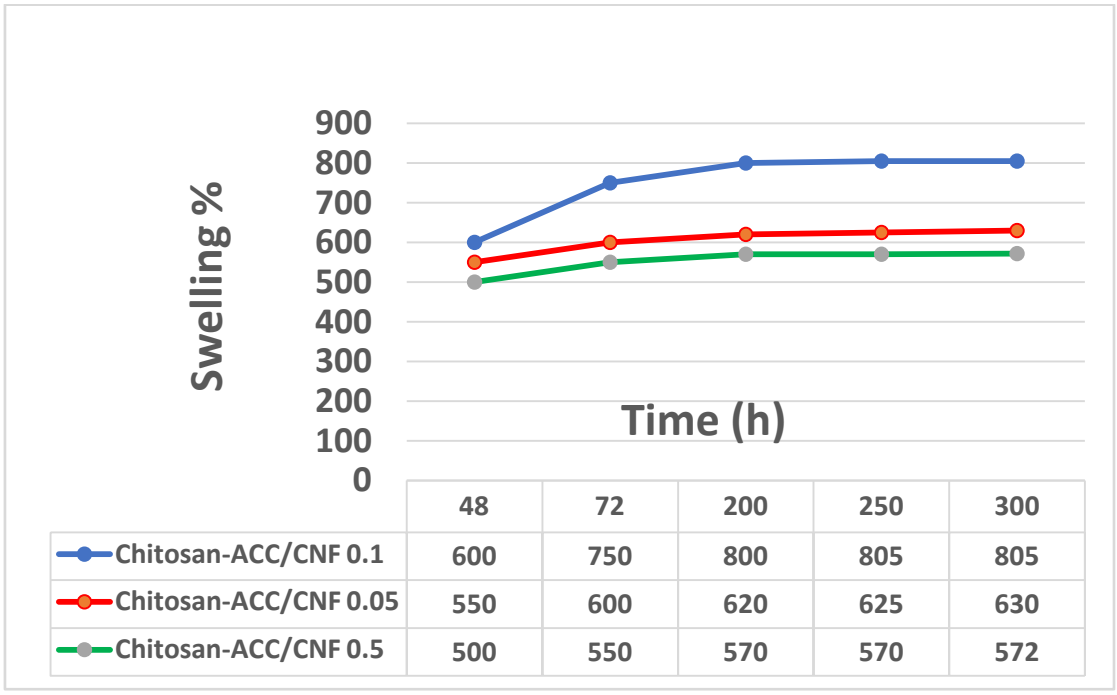

	48	72	200	250	300
Chitosan-ACC/CNF 0.1	600	750	800	805	805
Chitosan-ACC/CNF 0.05	550	600	620	625	630
Chitosan-ACC/CNF 0.5	500	550	570	570	572

Figure(6):Swelling behavior of different compositions of Chitosan-g-Poly(AAc)/CNF$_{0.1}$hydrogels at equilibrium.

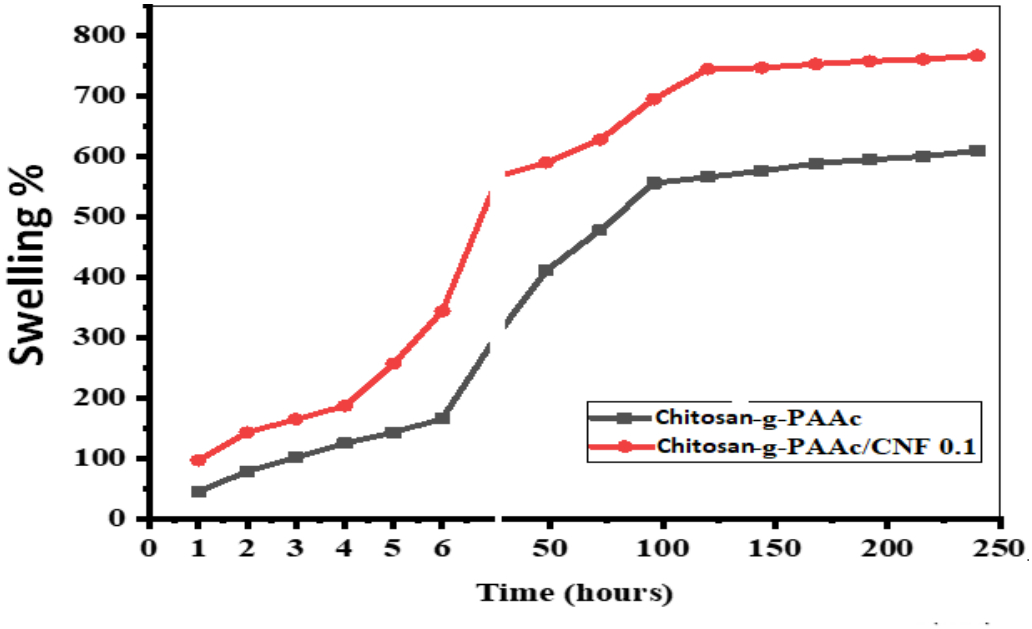

Figure (7): Swelling behavior ofChitosan-g-Poly(AAc)/CNF$_{0.1}$ and Chitosan-g-Poly(AAc) hydrogels against time.

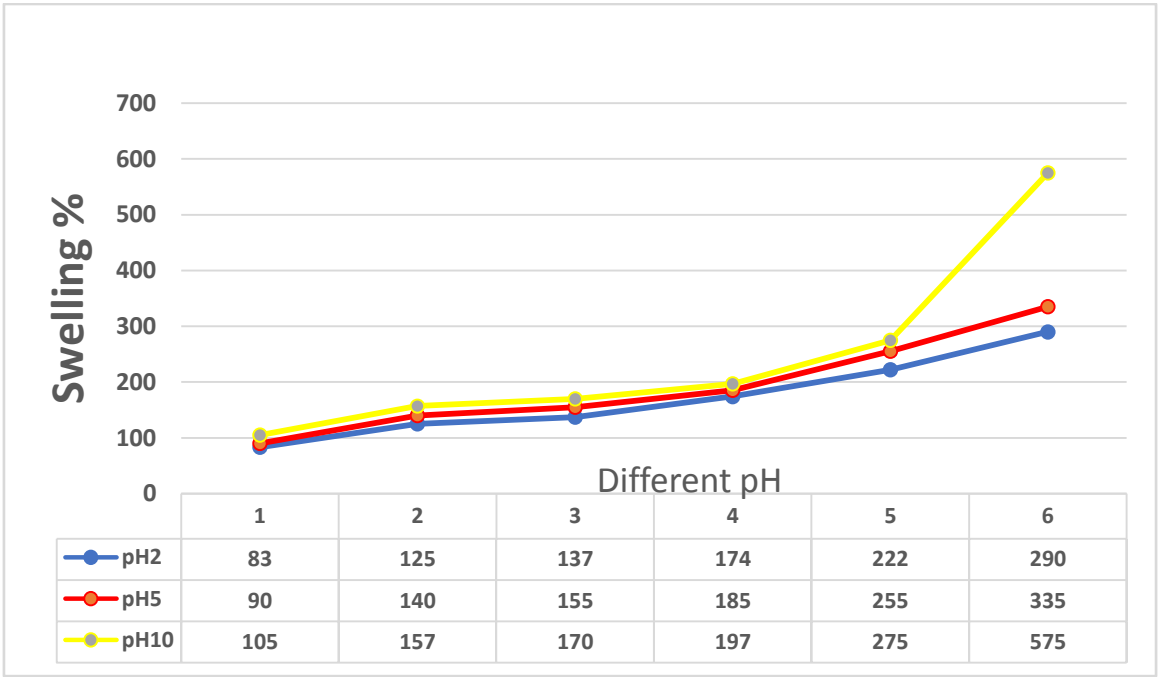

	1	2	3	4	5	6
pH2	83	125	137	174	222	290
pH5	90	140	155	185	255	335
pH10	105	157	170	197	275	575

Figure(8):Swelling behavior of Chitosan-g-Poly(AAc)/CNF$_{0.1}$hydrogel at different pH.

Fourier Transform Infrared Spectroscopy Analysis(FT-IR).

The FTIR spectra of pure Chitosan, Chitosan-g-Poly(AAc), and Chitosan-g-Poly(AAc)/CNF$_{0.1}$ nanocomposite are displayed in Figure 5. Peaks around 3249 cm1 and 1640 cm1 were visible in the spectrum of pure Chitosan due to intramolecular OH-group bending and stretching vibrations, which both occurred as broadband vibrations**(Vizireanu et al., 2018)**.

Also, a major peak at 2933 cm^{-1}attributedto C–H stretching, while C–H wagging noted at (~1344 cm^{-1}) **(Sarkaret al., 2020)**. C-O-C groups are associated with the peak at 1005 cm-1. The band at 1435 cm1 corresponds to stretching mode of the carboxylate (COO^-) anions, and it confirms the presence of the strong peak at 1700 cm1 in the spectrum of the Chitosan-g-Poly(AAc) hydrogel shown in Figure.5b. This peak is caused by asymmetric stretching in the carboxylic group of acrylic acid (AAc). These findings demonstrated

that the carboxylic and carboxylate groups of hydrogels were positively affected by the grafting of AAc onto the Chitosan, improving the hydrogels' ability to swell. When CNF was added to the matrix, Figure.5c revealed that the cellulose's distinctive peaks had been joined by a few further peaks at 1000 and 920 cm-1., were the result of vibrational actions of C–O–C and stretching of C–C and C–O ofpyrin ring.

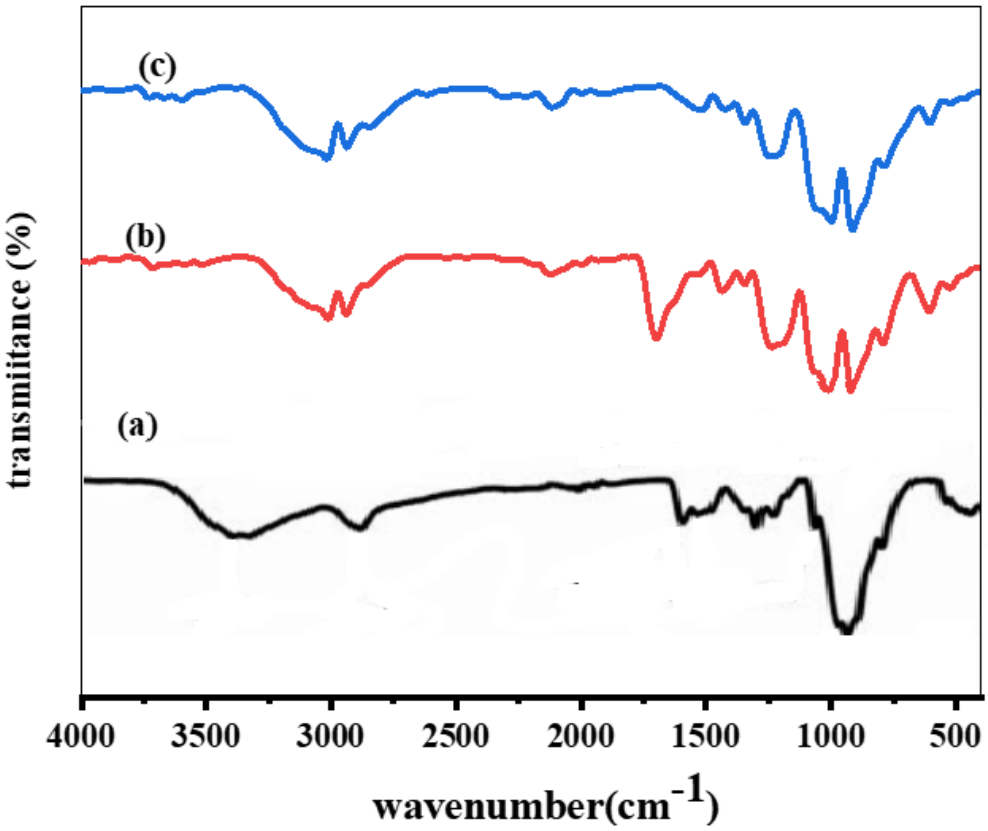

Figure(9):FTIR spectroscopic analysis of (a) Pure Chitosan, (b) Chitosan-g-Poly(AAc), and (c)Chitosan-g-Poly(AAc)/$CNF_{0.1}$

Surface and topography investigations

Scanning electron microscope (SEM)

Various hydrogels' morphology and pore size are visible under the scan electron microscope. The results of our study's experiments support the porous structure that had developed due to the stretched structure after the freeze-dried action of the hydrogel samples. Figures 10 (a), (b), and (c) show images of Chitosan-g-Poly(AAc) at various pH levels. At pH 2, the hydrogels are not smooth and have numerous pores, while at pH 5, they are smooth **(Chiulan, et al., 2021)**, Contrary to pH 10, the globules were dimensioned. Due to the COOH group's responsiveness to the pH, the surface morphology changes to a flaky structure with numerous pores. In an acidic environment, the carboxylic group protonates up to pH 4.6. Therefore, a further rise in pH causes deprotonation of the carboxylic group. New holes and voids can form due to the negatively charged carboxylate ions' repulsion, which enhances the equilibrium of the swelling**.**

Chitosan-g-Poly(AAc)/$CNF_{0.1}$ hydrogels are represented in Figure 10 (d), (e), and (f), respectively. The addition of CNF in Figure 6d increases the cross-linking density at pH 2, which typically results in a narrower pore structure. In Figure 6e, the hydrogels are not smooth at pH 5, and pores and globules begin to appear as the pH rises. In Figure 8f, the pores on the cracked surface have transformed from minor to big structure, and the dispersal has become uneven. These holes resulted from the pulling out of CNFs when the negatively charged carboxylate ions of AAc of the composite of chitosan-g-PAAc/CNF 0.1 were repelled**(Dhar et al., 2015)**.

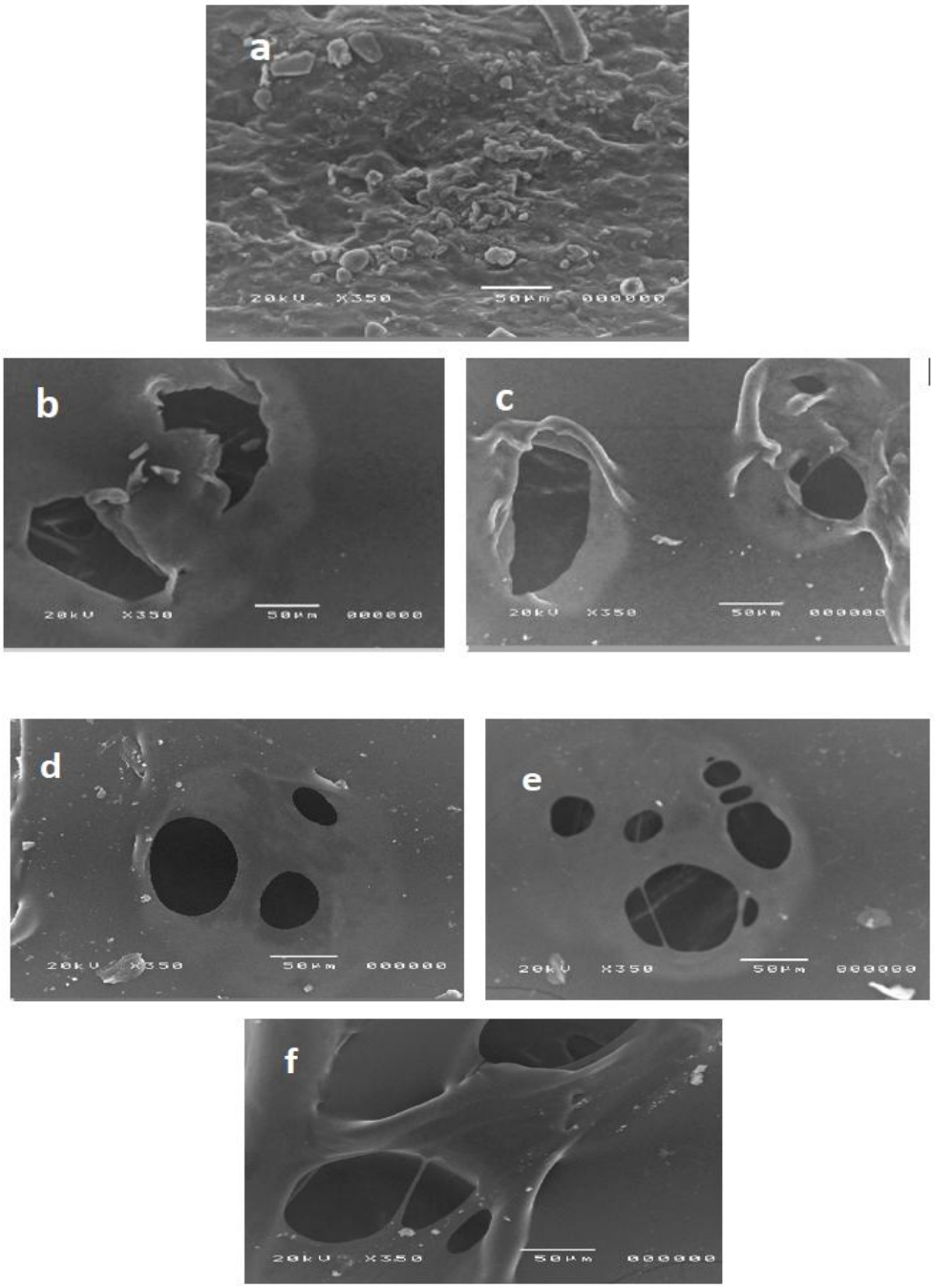

Figure(10):Scanning electron micrograph of Chitosan-g-Poly(AAc)(a, b, and c) andChitosan-g-Poly(AAc)/$CNF_{0.1}$ (d, e, and f).

Transmission electron microscope (TEM) imaging

Figure (7) shows images of the cellulose nanofibers as a blank (a). CNF exhibited a "narrow, two-rod-like structure and exhibited a grid-like structure, while the Chitosan-g-Poly(AAc)/$CNF_{0.1}$ (b) shown particles accumulation that possibly attributed to the existence ofelectric double layer on the nanoparticles surfaces which generates an electrostatic attraction force between nanoparticles**(Albukhaty et al., 2020)**. In addition, the diameters of both Chitosan-g-Poly(AAc)/$CNF_{0.1}$ and CNF nanoparticles were below 100 nm, as requested.Cellulose nanofibers, Chitosan-g-Poly(AAc)/$CNF_{0.1}$ exhibited a slight decrease in particle size. These newmodificationsmay be endorsed to the intramolecular cross-linked construction enriched with irradiation induced polymerization, causing a remarkable reduction in particle sizes**(Pasanphan et al., 2010)**. TEM findings data support our XRD outcomes.

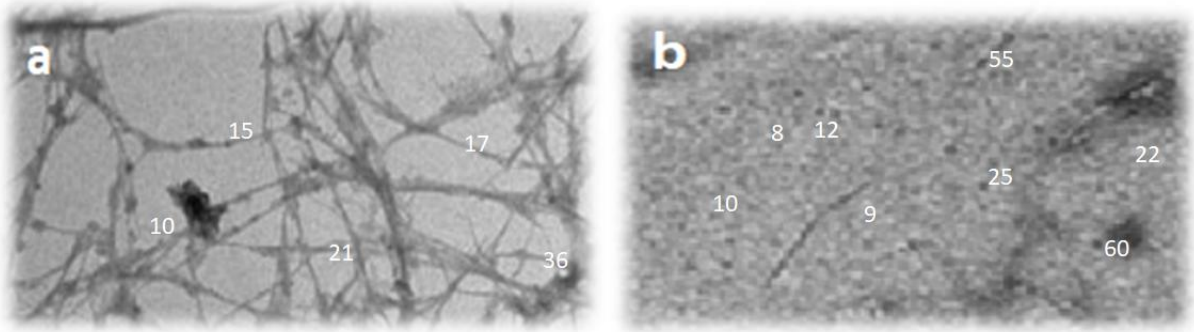

Figure (11):TEM images of (a) CNFcellulose nanofibers and (b)Chitosan-g-Poly(AAc)/CNF$_{0.1}$at 20kGy irradiation dose.

Thermal stability

TGA and DTG were used to identify thermal stability of Chitosan-g-Poly(AAc)/CNF$_{0.1}$ and Chitosan-g-Poly(AAc) composites and compare them with the original Poly(AAc) thermal properties. The results are shown in Figure12. It was noted that for Chitosan-g-Poly(AAc)andPoly(AAc), thermal degradation done in two phases but in contrary for Chitosan-g-Poly(AAc)/CNF0.1 composite, the thermal degradation was carried out through three phases. The initial decomposition phase was represented at 285.9 °C for Chitosan-g-Poly(AAc) and 245.5 °C,for Poly(AAc), due to the eradication of water. The next 2nd decomposition phase performed at 425.9 °C andat 385.4 °C for Poly(AAc),due to the decomposition of the main backbone.ForChitosan-g-Poly(AAc)/CNF$_{0.1}$, the initial decomposition phase was recorded at 246.5°C due to the eradication of water. The second decomposition phase shownat 302.5°C due to eradicating of theside branches groups. The 3rddecomposition phase is the main phase wasshown at 443.5°C due to the decomposition of themain structure. 1.3 % the percentage of residue Poly/Chitosan-g-AAc composite and 1.6 %Poly(AAc), on the other hand the residue of Chitosan-g-Poly(AAc)/CNF$_{0.1}$nanocomposite was 22.3%. The outcomes indicates that theChitosan-g-Poly(AAc)/CNF$_{0.1}$ nanocomposite poses higher thermal stability compared with the Poly/Chitosan-g-AAc compositeandPoly(AAc) as well, this is due to the impact of CNF addition**(Neto et al., 2021)**.

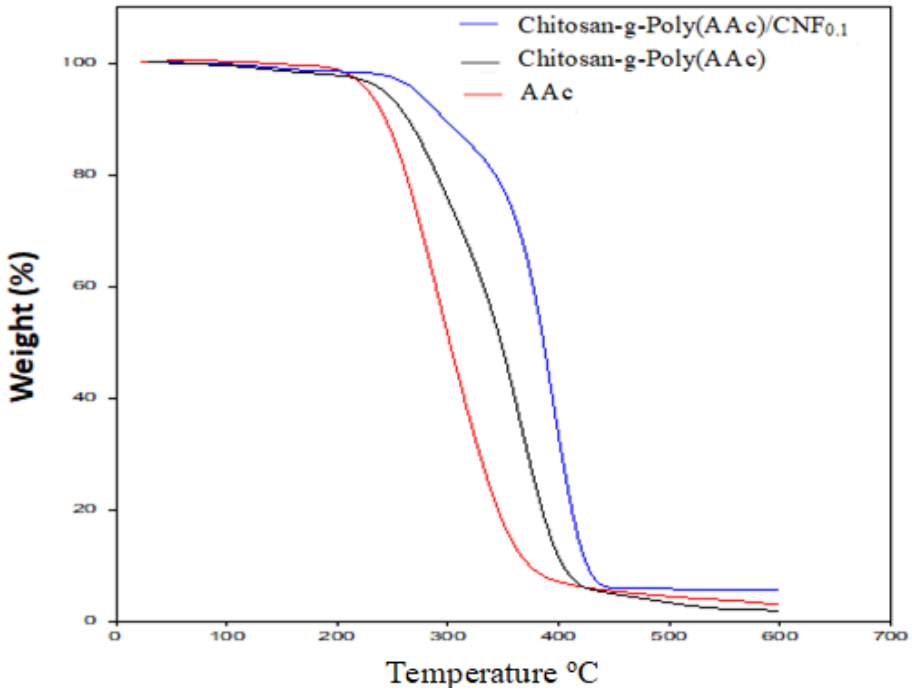

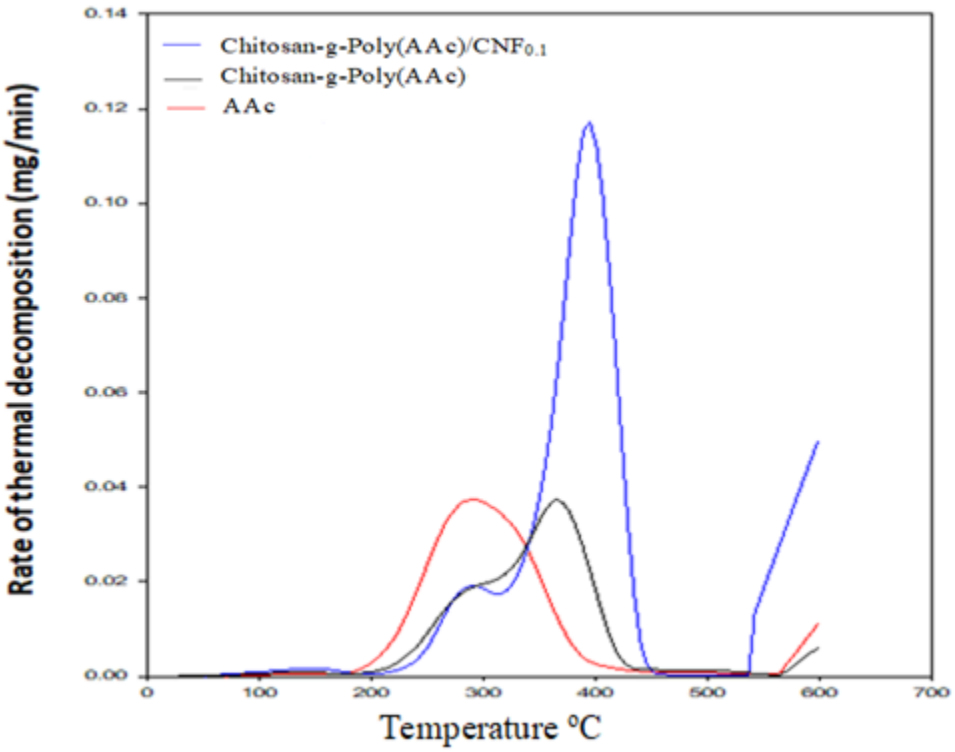

Figure(12):TGA and DTGcurves ofPoly(AAc),Chitosan-g-Poly(AAc) and Chitosan-g-Poly(AAc)/$CNF_{0.1}$.

Adsorption study

Impact of time on the removal percent ofCd^{2+}Ions.

Until the adsorption equilibrium, the removal percentage increased gradually. Metal ion uptake into the surface of the prepared nanocomposites increased along with the exposure time until it reached equilibrium**(Sayed et al., 2022).**

The adsorption performance is directly related to the possible adsorption sites on the surface. ICP-OES outcomes represent a potential adsorption affinity of Chitosan-g-Poly(AAc)/$CNF_{0.1}$ nanocomposite compared with Chitosan-g-Poly(AAc) composite due to the presence of (cellulose nanofibers) as represented in Figure(13). CNFs enhanced the surface properties and increased the specific surface area of the prepared nanocomposite which turned the surface to have more accessible sites for more adsorption capacity performance so more Cd^{2+}ions will be trapped. The slightly rate of adsorption is affected by the electrostatic interactions between the adsorbed Cd^{2+} ions on the surface of the prepared nanocomposites as time goes on and also will obstructs the diffusion rate of Cd^{2+} ions into the prepared nanocomposites matrix**(Ketsela et al., 2021).** Active sites have become engaged by time, and the standing vacant sites have become challenging to access due to physical restrictions**.**

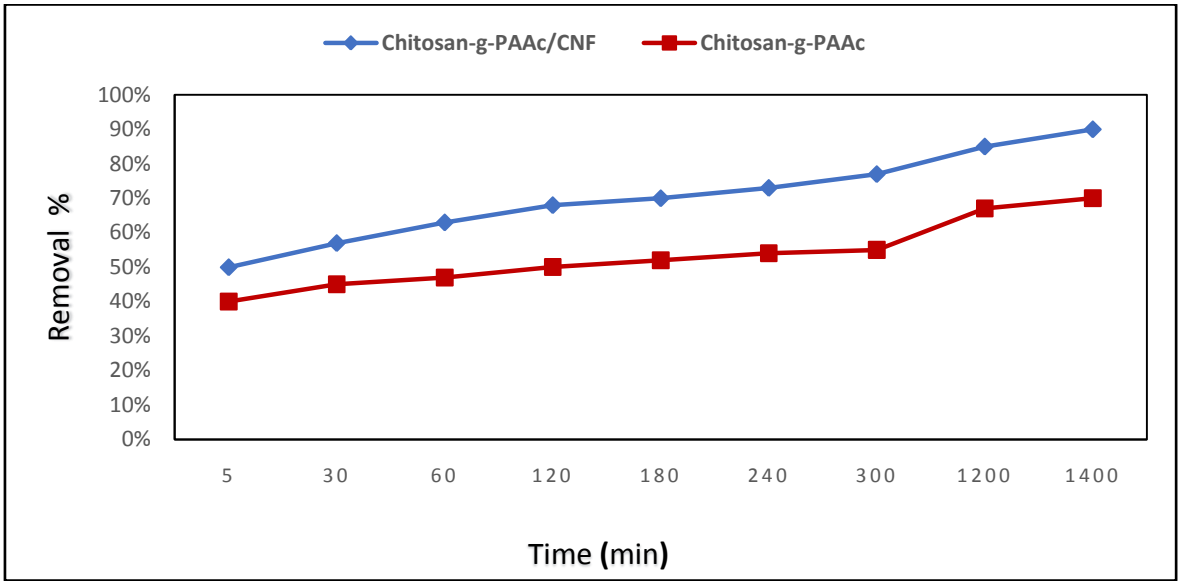

Figure(13):Impact of Time on the removal % of Cd (II) for Chitosan-g-Poly(AAc)/$CNF_{0.1}$and Chitosan-g-Poly(AAc).

Impact of Temperatureonthe removal percent of Cd^{2+}Ions.

Figure (14), which demonstrates the effects of temperature on the removal percentage of Cd^{2+} ions forChitosan-g-Poly(AAc) composite and Chitosan-g-Poly(AAc)/$CNF_{0.1}$nanocomposites. Three different temperatures were applied. According to the outcomes, the percentage of Cd^{2+} ions removed improved as the temperature rose from 25 to 60 °C. By altering the molecular interactions and solubility, the temperature impacts the rate of adsorption. The movement of Cd^{2+} ions increases with temperature. Because the hydrogel surface has been modified to create new, vacant active sites or the slow absorption process has been speed up **(Zhang et al., 2019)**.

Additionally, it offers the "activation-energy" required to crack the lattice-structure and allow the adsorbent access. As the temperature rises, so do the rates of absorption and diffusion, and vice versa. As the rate of adsorption increases, the control over the diffusion velocity decreases.

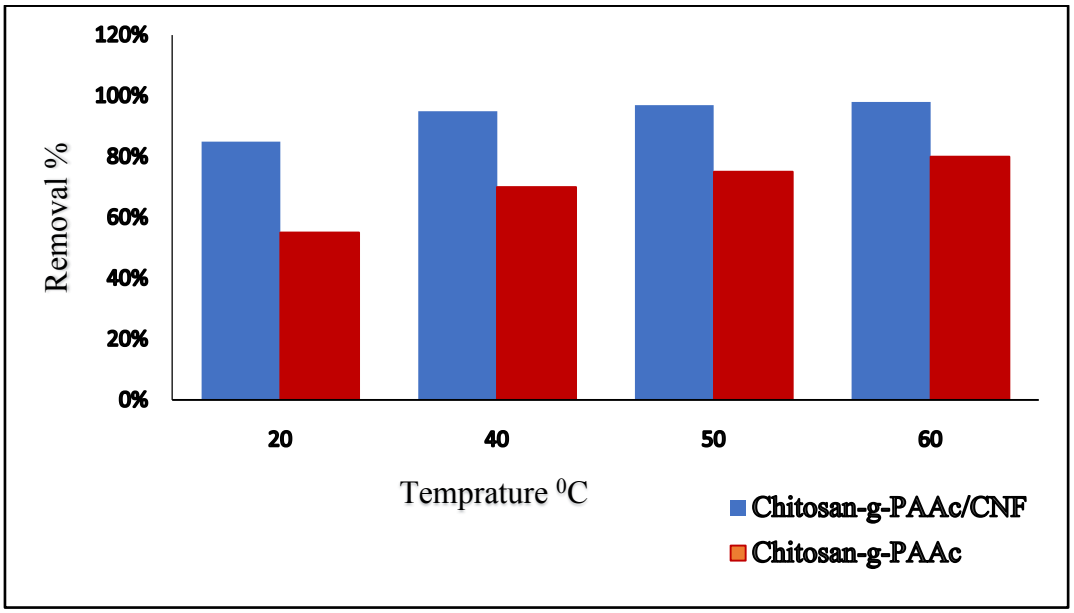

Figure (14):Effect of Temperature on the removal % of Cd (II) for Chitosan-g-Poly(AAc)/$CNF_{0.1}$,and Chitosan-g-Poly(AAc).

IV. Conclusion

The prepared composite of Chitosan-g-Poly(AAc), and the nanocomposite of Chitosan-g-Poly(AAc)/$CNF_{0.1}$were created using varying contents of chitosan, PAAc and CNFsvia an electron beam (EB) at a 20 kGy irradiation dose. The properties of Chitosan-g-Poly(AAc)/$CNF_{0.1}$are enhanced by the presence of CNFs in the polymeric matrix. The Prepared nanocomposite of Chitosan-g-Poly(AAc)/$CNF_{0.1}$displayed the highest swelling capacity, the highest thermal stability, and also the highest adsorption capacity. The maximum amount of Cd (II) that can be removed by the Chitosan-g-Poly(AAc)/$CNF_{0.1}$hydrogel is 94%. The prepared Chitosan-g-Poly(AAc)/CNFnanocomposite formula is suitable to remove various metal ions and heavy metals from the aquatic solutions.

Research Funding

The author received no financial support for the research, authorship, and/or publication of this research paper.

Author's Contribution

The author designed the study along with writing the research paper in line with the Journal's requirements.

Conflict of Interests: Disclaimer

The author of this research paperis solely responsible for the content thereof. Data, ideas and opinions presented herein do not necessarily represent the corporate views of the Saudi Arabian Oil Company.

References

[1]. Ahmad, M.A., Ahmad Puad, N.A., Bello, O.S., (2014) Water Res. Ind.,(6), 18–35.
[2]. Albukhaty, S., Al-Bayati, L., Al-Karagoly, H., Al-Musawi, S., (2020) Preparation and characterization of titanium dioxide nanoparticles and in vitro investigation of their cytotoxicity and antibacterial activity against Staphylococcus aureus and Escherichia coli. Anim. Biotechnol.,1–7.
[3]. Bretel, G., Rull-Barrull, J., Nongbe, M.C., Terrier, J.-P., Le Grognec, E., Felpin, F.-X., (2018) Hydrophobic Covalent Patterns on Cellulose Paper through Photothiol-X Ligations. ACS Omega, (3), 9155–9159.
[4]. Bryan, T., Omar, G., Pascale, Ch., Michael F., (2017) Poly(Poly(Ethylene Glycol) Methyl Ether Methacrylate) Grafted Chitosan for Dye Removal from Water Processes, (5), 12.
[5]. Chang, M., Liu,X., Wang,X., Peng,F., Ren,J.,(2021) Mussel-inspired adhesive hydrogels based on biomass-derived xylan and tannic acid cross-linked with acrylic acid with antioxidant and antibacterial properties. Journal of Materials Science, 56**,** 14729-14740.
[6]. Chiulan, I., Panaitescu, D.M., Radu, E.-R., Vizireanu, S., Sătulu, V., Bi¸tă, B., et al., (2021) Influence of TEMPO oxidation on the properties of ethylene glycol methyl ether acrylate grafted cellulose sponges. Carbohydr. Polym., (272), 118458.
[7]. Dhar, P., Bhardwaj, U., Kumar, A., Katiyar, V., (2015) Poly (3-hydroxybutyrate)/cellulose nanocrystal films for food packaging applications: Barrier and migration studies. Polym. Eng. Sci., (55), 2388–2395.
[8]. Faheem, U., Muhammad, B. O., Fatima, J., Zulkifli, A., Hazizan, M., (2015) Classification, processing and application of hydrogels: A review, Materials Science and Engineering, C 57 414–433.
[9]. Gharekhani, H., Olad, A., Mirmohseni, A., Bybordi, A., (2017) Superabsorbent hydrogel made of NaAlg-g-poly(AA-co-AAm) and rice husk ash: Synthesis, characterization, and swelling kinetic studies. Carbohydr. Polym. ;168:1–13. doi: 10.1016/j.carbpol.2017.03.047.
[10]. Gonçalves, J.O., Santos, J.P., Rios, E.C., Crispima, M.M., Dottob, G.L., and Pinto L.A.A., (2017) Development of ChitosanChitosan based hybrid hydrogels for dyes removal from aqueous binary system Journal of Molecular Liquids, 225, 265–270.
[11]. Gupta, V.K., Atar N., Yola M.L., Üstündağ Z., Uzun L., (2014) Water Res.,(48), 210–217.
[12]. Huq, T., (2012) Nanocrystalline cellulose (NCC) reinforced alginate based biodegradable nanocomposite film. Carbohydrate polymers,(90), 1757–63.
[13]. Iram, T., Zaheer, A., Aamir, A., Muhammad, M., Sadaqat, A., Anam, A., (2019) Adsorptive removal of acidic dye onto grafted ChitosanChitosan: A plausible grafting and adsorption mechanism, International Journal of Biological Macromolecules,(136), 1209–1218.
[14]. Jayaramudu, T., Ko, H.-U., Zhai, L., Li, Y., Kim, J., (2017) Preparation and characterization of hydrogels from polyvinyl alcohol and cellulose and their electroactive behavior. Soft Mater.;15:64–72. doi: 10.1080/1539445X.2016.1246458.
[15]. Ketsela, G., Animen,Z., Talema,A.,(2021) adsorption-of-lead-ii-cobalt-ii-and-iron-ii-from-aqueous-solution-by-activated-carbon-prepared-from-white-lupine-gibito. Journal of Thermodynamics & Catalysis, 11.
[16]. Khawar, A., Aslam, Z., Javed, S., Abbas A., (2018) Chem. Eng. Commun., 1–13.
[17]. Mahamad, M.N., Zaini, M.A., Zakaria, Z.A., (2015) Int. Biodeterior. Biodegradation, 102, 274–280.
[18]. Manas, D., OvsikM., MizeraA., ManasM., HylovaL., Bednarik M., et al., (2018) The Effect of Irradiation on Mechanical and Thermal Properties of Selected Types of Polymers. Polymers, 10**,** 158.
[19]. Neto, J.S., de Queiroz, H.F., Aguiar, R.A., Banea, M.D., (2021) A Review on the Thermal Characterisation of Natural and Hybrid Fiber Composites. Polymers, 13, 4425.
[20]. Pasanphan, W., Rimdusit, P., Choofong, S., (2010) Systematic fabrication of chitosan nanoparticle by gamma irradiation. Radiat Phys Chem.,79, 1095–1102.
[21]. Randhawa, A., Dutta, S.D., Ganguly, K., Patil, T.V., Patel, D.K., Lim, K.T., (2022) A Review of Properties of Nanocellulose, Its Synthesis, and Potential in Biomedical Applications. Appl. Sci., 12, 7090.
[22]. Samiullah, M., Aslam, Z., Rana, A.G., Abbas, A., Ahmad, W., (2018) Water Air Soil Pollut., 229, 113.
[23]. Sarkar, N., Sahoo,G., Swain, S. K., (2020) Graphene quantum dot decorated magnetic graphene oxide filled polyvinyl alcohol hybrid hydrogel for removal of dye pollutants. Journal of Molecular Liquids, 302**,** 112591.

[24]. Saravanan, R., Karthikeyan, N., Gupta, V.K., Thirumal, E., Thangadurai, P., Narayanan, V., et al., (2013b) Mater. Sci. Eng., C 33, 2235–2244.
[25]. Saravanan, R., Gupta, V.K., Mosquera, E., Gracia F., (2014a) J. Mol. Liq., 198, 409–412.
[26]. Saravanan R., Gupta V.K., Narayanan V., Stephen A., Taiwan J., (2014b) Inst. Chem. Eng., 45, 1910–1917.
[27]. Sayed, A., HanyF., Abdel-RaoufM. E.-S., Mahmoud G. A.,(2022) Gamma irradiation synthesis of pectin- based biohydrogels for removal of lead cations from simulated solutions, Journal of Polymer Research, 29**,** 372.
[28]. Sokker, H., Ghaffar,A. A., Gad,Y.,Aly,A.,(2009) Synthesis and characterization of hydrogels based on grafted ChitosanChitosan for the controlled drug release. Carbohydrate polymers, 75**,** 222-229.
[29]. Vizireanu, S., Panaitescu, D.M., Nicolae, C.A., Frone, A.N., Chiulan, I., Ionita, M.D., et al., (2018) Cellulose defibrillation and functionalization by plasma in liquid treatment, Sci. Rep., 8, 15473.
[30]. Yang, J., Han, C., Zhang, X., Xu, F., Sun, R., (2014) Cellulose Nanocrystals Mechanical Reinforcement in Composite Hydrogels with Multiple Cross- inks : Correlations between Dissipation Properties and Deformation Mechanisms. macromolecules, 47, 4077–4086.
[31]. Zahir, A., Aslam, Z., Kamal, M.S., Ahmad ,W., Abbas, A., Shawabkeh, R.A., (2017) J. Mol. Liq., 244, 211–218.
[32]. Zhang, W., Hu,L., Hu,S. Liu,Y.,(2019) Optimized synthesis of novel hydrogel for the adsorption of copper and cobalt ions in wastewater. RSC advances, 9**,** 16058-16068.